

Design of a 3d printed non-linear vibration energy harvester using electromagnetic induction.

Hashem Elsaraf^{1*}, Chung Ket Thein², Mohsin Jamil³

¹Energy Systems Engineering, Faculty of Engineering, Memorial University of Newfoundland, Newfoundland, Canada

²Department of Aerospace, Faculty of Science and Engineering, University of Nottingham, Ningbo, China

³Department of Electrical Engineering, Faculty of Engineering, Memorial University of Newfoundland, Newfoundland, Canada

[*hasmaelsaraf@mun.ca](mailto:hasmaelsaraf@mun.ca)

Abstract—New improvements in electronics have resulted in ultra-low power wireless sensors (requiring only a few microwatts of power) optimal for Internet of Things applications. These devices, however, are powered by depletable batteries, which need to be changed, making them less effective. Therefore, vibration energy harvesters have been developed as a source of power for these sensors and to recharge their batteries. The majority of the initial research in this field concentrated on resonant (linear) vibration harvesters. More recently, researchers have started exploring non-linear vibration harvesters as they provide higher power and wider bandwidth. The aim of this paper is to produce a simple 3D printed non-linear vibration energy harvester, which applies electromagnetic induction and magnetic levitation to transform vertical vibrations into electricity. Some improvements that can better the performance of a non-linear harvester are investigated. Comparisons are made between different topologies based on power, bandwidth and power density. Monostable hardening (double upper magnet double lower magnet topology) showed the best results (+138.1% power density increase and +233.3 maximum power increase). A novel improvement on the power produced by multipole magnets is tested on CST studio; the results showed that the addition of two 1mm thick plates made of steel above and below the moving magnet could improve power by increasing the peak B-field by 9%. Experimentally testing this improvement produced an average voltage increase of 11.73% and power increase of 24.94%.

Keywords: *Vibration Energy Harvesting, Non-Linear, Bistable, Monostable, Magnetic Levitation, Electromagnetic Induction, CST Studio, Duffing Oscillators.*

I. INTRODUCTION

There are many sources of unused energy in nature that are sustainable and renewable. However, they mostly lay in ambience and are not used. These sources include wind, water, geothermal, sunlight, and vibration energy. Vibration energy has attracted a lot of research attention as of late. It is a renewable mechanical energy that can be converted into electrical energy. The energy

produced from this transduction can be used to directly power electronics or put in storage for future usage. While there are various methods for converting vibration energy to electrical energy such as piezoelectric, electrostatic, and magnetostrictive, electromagnetic induction is the simplest and most cost-effective [1].

While linear vibration harvesters have received the majority of the research in this topic, they notoriously suffer from narrow bandwidth and have a high susceptibility to mistuning. Linear harvesters can perform well enough if a priori knowledge of the exact excitation frequency exists and if that frequency does not vary, but this is not the case for practical scenarios where most vibrating sources have a frequency varying spectrum. This limits the application of linear vibration harvesters. For this reason, a large body of continuing research has focused on the inclusion of non-linearities to improve the performance of vibration harvesting [2].

This study aims to produce improvements in the performance of non-linear magnetic levitated electromagnetic induction vibration energy harvester. Therefore, the main objective of this study is to improve the power of the designed device. This is initially achieved by using a duffing oscillator and multipole magnets as the moving mass. To decide on the best type of duffing oscillator to use the three types of duffing oscillator (bistable, monostable softening and monostable hardening) are created and compared. This is accomplished through the introduction of different magnet topologies. Once the best topology is selected, further efforts to improve the device are applied. The efforts will mainly focus on improving power since the use of a non-linear device inherently offers an improved bandwidth.

II. METHODOLOGY AND APPARATUS

A. Shaker parameters

The Electromagnetic shaker EMS-050 was used for this research. In order to conduct any experiment using it, the frequency range, acceleration, and sweeping speed values must be selected. Frequencies from 6 to 40 Hz were used (low frequency region) [5]. Accelerations from 1g to 5g were used since recent research has shown the vibrations from different

sources such as human running and train passing could reach up to 5g acceleration [4]. Below 1g acceleration the device behaved as a linear device due to the critical input threshold [2]. The sweeping speed is set at the lowest value 0.1 oct/min to increase accuracy.

B. Proposed device design

The proposed device is designed on the 3D CAD software Revit AutoDesk printed using Ultimaker 2 go. The device is made from PLA (polylactic acid). However, since PLA has a high friction coefficient [6], the device is further prepared by removing any impurities using sandpaper, and a layer of petroleum jelly is applied. The petroleum jelly serves as a lubricant and lowers the friction between the moving magnet and the inner walls of the device. The magnets used are grade N35 neodymium permanent magnets. Each magnet has the dimensions 25x10x5 (length, width, thickness) and remanence (B_r) value of 1.2 teslas. The device is finalized by wrapping a 0.3mm enameled copper coil around it.

The device is equipped on the electromagnetic shaker and the free ends of the coil are next connected to the Centrand Boile A Decades De Resistance DRD08 (resistance decade box) and the Data acquisition unit which is connected to the computer.

The results of the experiments are obtained on the computer using the software LabVIEW. This file is then opened with MATLAB, where results are converted from the time domain to the frequency domain.

A height of 10 cm was chosen as the height of the design since, through experimentation, the largest separation distance between the magnets where the upper and lower magnets could still affect the middle magnet was found to be 5 cm. The final design has 26mm internal length (25mm was the magnet length leaving 1mm as tolerance), and the final width is 11mm (1mm width tolerance). The total device volume is 51.5 cm³. Even though size minimization is not an explicit goal of this work, the proposed device is small enough to fit in one's hand.

To increase the stability of the device and to counter any chance of collapsing, 1mm thick support beams were created on both sides of the device. In between the support beams and the device wall are 1.5 mm coil slots. The device wall is 3mm thick at the body and 0.5 mm thick at the coil slot. Since the diameter of the coil is 0.3mm, and the coil slot is 1.5mm wide, and 15mm in height, 4-5 turns of the coil can be wound horizontally for every 0.3 mm of coil slot height. This makes the total number of possible coil turns 180-225. For this work, only 150 turns are used.

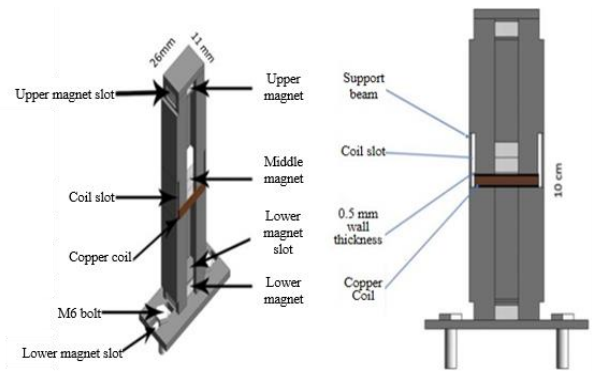


Figure 1. Final device schematic (5 magnets, one upper, one lower and three as the floating magnet).

III. RESULTS AND DISCUSSION.

A. Monostable

Five upper and lower magnet topologies are studied. The resulting five monostable configurations are single upper magnet single lower magnet topology (sumslm); single upper magnet double lower magnets topology (sumdlm); double upper magnets double lower magnets topology (dumdlm); single lower magnet no upper magnet topology (slmnum); double lower magnets no upper magnet topology (dlmnum).

In sumslm, 5 magnets are utilized, in sumdlm 6 magnets are utilized, in dumdlm 7 magnets are utilized, in slmnum 4 magnets are utilized, in dlmnum 5 magnets are utilized. The number of magnets utilized is significant for power density calculations. These topologies are examined at accelerations ranging from 1 g to 5 g using a 150-turn coil hand wrapped around the outside of the device, which is 4mm away from the moving magnet. Results and conclusions acquired are used to guide further stages of this work.

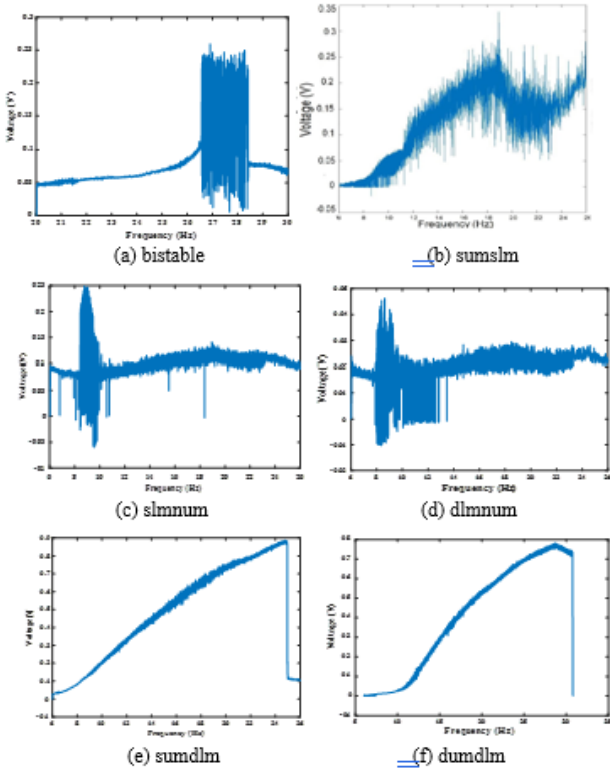


Figure 2. Frequency response curves of the different magnet topologies at 5g acceleration. (a) bistable topology. (b) sumslm topology. (c) slmnum topology. (d) dlmmum topology. (e) sumdlm magnet topology. (f) dumdlm magnet topology.

1) Double upper magnets double lower magnets topology

The frequency response curves for the dumdlm configuration exhibits the best performance out of all the different configurations. The bandwidth of the curve increases as the input acceleration increases saturating at 35 Hz bandwidth at 4g acceleration. The voltage in dumdlm also saturate at 4g, similar to the sumdlm configuration. The highest voltage recorded of all the five configurations (1 volt) can be seen here for the 4g and 5g curves (Table I) (Fig. 2f).

When a monostable hardening device is exposed to a frequency up-sweep, the output voltage increases up to a maximum point after which it suddenly drops to a lower amplitude. On the other hand, when the monostable device is exposed to a frequency down-sweep the voltage slowly increases until it reaches a certain frequency then it suddenly jumps up to a higher value. As the frequency further decreases the amplitude of the voltage gradually decreases as well, resulting in the same curve as the one obtained from the frequency up-sweep. It was also found out that the jump up and jump down points are largely influenced by the degree of non-linearity. Another note was that decreasing the separation distance between the moving magnet and the lower and upper magnets increases the magnetic stiffness and therefore increases the degree of non-linearity [4].

2) Monostable results summary

TABLE I. Bandwidth (Hz) and Peak Voltage (V) comparison between the five monostable configurations at accelerations 1g to 5g.

		1g	2g	3g	4g	5g
sumslm	Bandwidth	4	11	13	35	35
	Peak Voltage	0.045	0.16	0.2	0.25	0.3
sumdlm	Bandwidth	13	16	14	19	21
	Peak Voltage	0.66	0.85	0.8	0.88	0.89
dumdlm	Bandwidth	12	20	22	25	23
	Peak Voltage	0.7	0.9	0.94	1	0.98
slmnum	Bandwidth	2	1	2	2	2
	Peak Voltage	0.25	0.12	0.2	0.25	0.25
dlmmum	Bandwidth	2	2	2	2	2
	Peak Voltage	0.1	0.035	0.04	0.04	0.04

B. Power density

In this work, the power density is calculated as power divided by magnet volume ($\mu\text{W}/\text{mm}^3$ of magnet volume). dlmmum and slmnum are not mentioned here as they have been omitted from further analysis. Since sumslm is the default configuration it is chosen as the reference point.

TABLE II. Five monostable configurations and bistable comparison for different performance metrics

Type	Power max (W)	Band width (Hz)	Power density ($\mu\text{W}/\text{mm}^3$)	Power Density % increase	Power % increase	Bandwidth% increase
sumslm	0.03	35	4.8	Reference	Reference	Reference
sumdlm	0.089	21	11.87	+147.2%	+196.6%	-40%
dumdlm	0.1	25	11.428	+138.1%	+233.3%	-28.57%
bistable	0.03	5	2.67	-44.44%	0%	-85%

Sumslm exhibited the highest bandwidth but displayed poor performance on maximum power and power density metrics. Sumdlm exhibited the best power density and second-best maximum power but came in third on the bandwidth category. In comparison dumdlm displayed the best maximum power, the second-highest power density, and was the second highest in the bandwidth category. Bistable had an overall poor performance and did not make the cut for further analysis. The best two configurations that made it to the final comparison are dumdlm and sumdlm, and the conclusion is that while sumdlm has a slightly higher power density improvement compared to the reference, the difference in power density improvement between sumdlm and dumdlm is only 9%, while the difference in the maximum power of dumdlm and sumdlm is 36.7%. Also, dumdlm has 11.43% better bandwidth when compared to the reference than sumdlm, hence dumdlm is picked as the best configuration that produces a delicate balance between the different performance categories.

One important note is that bistable performed poorly on power density compared to monostable, as can be seen in table II. This is because the device requires two extra bistable magnets in order for the system to function as a bistable system. It also exhibited low bandwidth. One advantage of bistable is that it generates the same output voltage over a certain range of frequencies compared to monostable hardening, which generates a different voltage for each frequency within its bandwidth. This can make a bistable harvester easier to process. Researchers have stated that up to a few years ago no literature had made a comparison between monostable and bistable [3]. However, the results of a later research paper demonstrated that there was no benefit in the power output of bistable harvesters over monostable harvesters. It was noted that bistable performed poorer than the reference system, while monostable performed better. However, these results are only valid for the four vibration profiles used [7].

Since for a monostable harvester there is no need for additional magnets in order for the device to achieve non-linearity, the total volume of the monostable device is usually smaller than a bistable device [8].

C. CST studio

A novel contribution is introduced in this section. It involves the addition of 1mm thin sheets of material in two configurations. The result of the simulation is used to guide further experimental studies. It should be noted that for magnetically levitated devices limited literature exists on the addition of material as proposed in this study.

1) Configurations

In this section, four materials in two configurations are studied. Polycarbonate (plastic), aluminum, copper and steel in the “in-between” and “up and down” configurations. In the “in-between” configuration, hereby dubbed as b-t, a 1mm sheet of material is placed between the first and second magnets and another sheet between the second and third magnets. In the up and down configuration, hereby dubbed as u&d, a 1mm sheet of material is placed on top of the first magnet and another sheet at the bottom of the third magnet (Fig. 3). The configurations are simulated on the finite element analysis software CST studio, and the flux density is measured at multiple measurement points (1, 1.3, 1.6, and 1.9 mm away from the moving magnet)

In fig. 4, the “in-between” and “up and down” configurations for steel are compared to the no added material configuration (default configuration) at the 1 mm away from the moving magnet measurement point. Table III summarizes the change in peak B-field for each configuration.

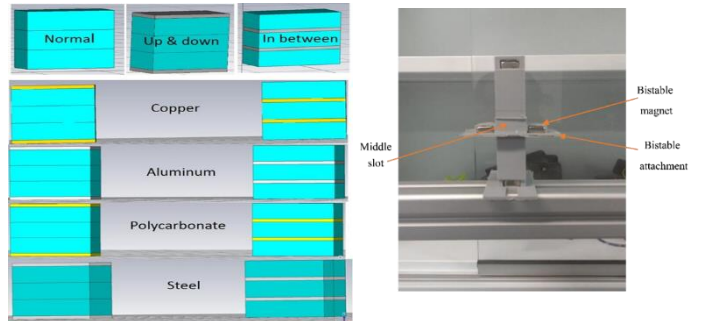


Figure 3. (a) The four materials (copper, aluminum, polycarbonate, steel) in the two configurations (up&down and in-between) (b) physical device

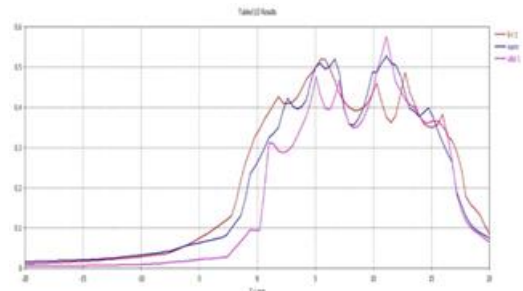


Figure 4. Steel comparison curves of up & down (pink) vs. in-between (red) vs normal (blue) at measurement point 1mm away from the magnet.

In a recent study by Munaz and Chung [9] it was found that as the number of flux changes increases, the power dramatically improves. Since steel up and down displayed the largest increase in peak B field as well as the largest increase in dB/dz (the change in amplitude of the magnetic field with respect to the z-axis), this justifies physical investigation and steel up and down is chosen for further experimentation in the following section.

TABLE III. Peak B-field comparison at measurement point 1mm away from the magnet (Polycarbonate and Copper results are the same as aluminum)

Case	Material	Peak B-field	% improvement over normal
Normal		0.528	
Up and down (u&d)	Steel	0.576	9.091%
	Copper	0.564	6.818%
	Aluminum	0.564	6.818%
	Polycarbonate (Plastic)	0.564	6.818%
In-between (b-t)	Steel	0.519	-1.725%
	Copper	0.506	-4.167%
	Aluminum	0.506	-4.167%
	Polycarbonate (Plastic)	0.506	-4.167%

D. Steel up & down experiment

Since the simulation of steel up and down on CST studio configuration is further tested in this section, through laser cutting technology, two pieces of stainless steel were obtained. The pieces had the dimensions 25x10x1 mm and since the material of the sheets is stainless steel, they are attracted to the moving magnet.

1) Steel 1g to 5g compiled

Fig. 5 is the compiled 1g to 5g curves for steel up and down configuration. These curves clearly show an increase in voltage and bandwidth as the acceleration level increases. The curve also show that the increase in voltage and bandwidth almost saturates at around 4g, and the difference between 4g and 5g is minuscule.

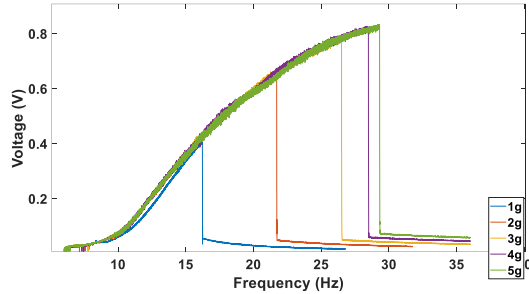


Figure 5. Steel up and down frequency response curves at acceleration 1g to 5g compiled.

2) Steel vs. normal (no added material) comparison

The important values from the curves of fig. 6 are summarized in table IV.

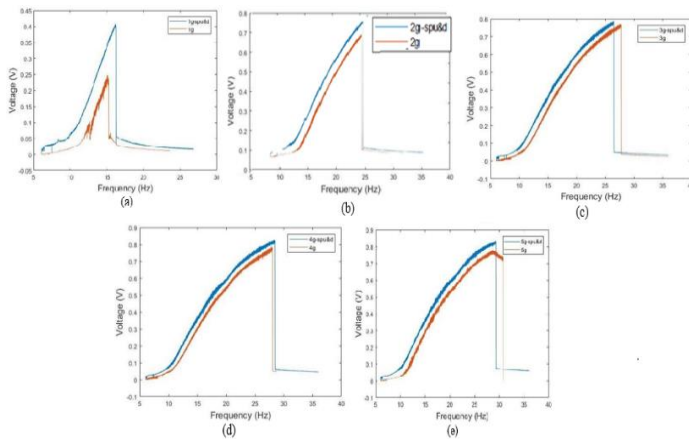


Figure 6. Steel up and down (blue) vs normal (orange) experimental curves at accelerations (a) 1g, (b) 2g, (c) 3g, (d) 4g, (e) 5g.

TABLE IV. Steel up and down versus normal voltage improvement

Acceleration	Normal Voltage (V)	Steel up and down Voltage (V)	% Voltage Improvement
1g	0.255	0.405	58.82%
2g	0.590	0.655	11.02%
3g	0.730	0.780	6.849%
4g	0.720	0.825	14.58%
5g	0.725	0.830	14.48%

TABLE V. Steel up and down versus normal power improvement

Acceleration	Normal Power (W)	Steel up and down Power (W)	% Power Improvement
1g	0.0650	0.1640	+152.31%
2g	0.3481	0.4290	+23.24%
3g	0.5329	0.6084	+14.168%
4g	0.5184	0.6806	+31.289%
5g	0.5256	0.6889	+31.069%

From table IV and table V we can observe that the largest improvement in voltage was recorded at 1g acceleration; it was a 58.8% improvement. The improvement in voltage for the 2g to 5g frequency response curves was between 6.849 and 14.583%. A possible explanation of why the improvement under 1g acceleration is so high could be that the effect of the two layers of steel is more pronounced in the low acceleration region. This is however contradicted by the value of the percentage improvements under 2g and 3g input accelerations, which are lower than the 4g and 5g accelerations. Therefore, this work will assume the values of the 1g curve as an outlier and will not be used for further analysis. By neglecting the value of the 1g curve, an average percentage improvement can be obtained by averaging the other four values, which results in an 11.73% voltage improvement, and by averaging the power improvement % values, we obtain the average power % improvement of 24.94%.

IV. CONCLUSION AND FUTURE WORK

In conclusion, a 3d printed non-linear magnetically levitated electromagnetic vibration energy harvester was designed in Revit Autodesk, it was printed using the Ultimaker 2 go 3D printer and tested using the vibration shaker EMS-050.

Five monostable and one bistable configuration were generated and compared. The monostable designs were achieved by varying the number of upper and lower magnets while the bistable system was attained by affixing a bistable attachment to the monostable device. A comparison between the different topologies was conducted based on the following performance categories: maximum power, percentage power increase, power density, percentage power density increase, bandwidth, and percentage bandwidth increase. Single upper magnet single lower magnet (sumslm) topology was used as the reference point as it is the starting/default configuration. As a result of the comparison, double upper magnets double lower magnets (dumdlm) topology was found to produce a delicate balance between sufficiently high bandwidth and robust power performance. Dumdlm was then subjected to further performance.

Then a simulation was performed on CST studio to experiment with the changes in the magnetic flux of the moving magnet as a result of adding 1mm thick sheets of four materials, i.e. copper, aluminum, steel, and polycarbonate. The materials were added one at a time in the “up and down” topology and the “in-between” topology. Adding steel in the up and down topology was found to generate a 9% improvement to the peak B field compared to the normal. Therefore, physical plates of steel were attached to the moving magnet in the up and down topology and tested. The results showed that, on average this addition improved the voltage of the harvested signal by 11.73% and the power harvested by 24.94%.

This work can be further expanded by studying different materials for the 1mm sheets introduced in this paper. Different

sheet thickness can be studied to find its effect on the output power. Case studies of specific real-life applications can be examined. Lastly, size minimization can be attempted while maintaining the same concepts developed in this work.

REFERENCES

- [1] L. Tang, Y. Yang, and C. Soh, "Broadband Vibration Energy Harvesting Techniques," in *Advances in Energy Harvesting Methods*, New York, NY, USA: Springer, 2013, pp.17-61. [Online]. Available:<https://www.researchgate.net/>
- [2] S. Chiacchiari, F. Romeo, D. M. McFarland, L. A. Bergman, and A. F. Vakakis, "Vibration energy harvesting from impulsive excitations via a bistable nonlinear attachment—Experimental study," *Mechanical Systems and Signal Processing*, vol. 125, pp. 185-201, Jun. 2019. DOI: 10.1016/j.ymssp.2018.06.058.
- [3] D. A. W. Barton, S. G. Burrow, and L. R. Clare, "Energy Harvesting From Vibrations With a Nonlinear Oscillator," *Journal of Vibration and Acoustics*, vol. 132, no. 2, Apr. 2010. DOI: 10.1115/1.4000809.
- [4] K. Suhaimi, R. Ramlan, and A. Putra, "A Combined Softening and Hardening Mechanism for Low Frequency Human Motion Energy Harvesting Application," *Advances in Acoustics and Vibration*, vol. 2014, pp. 1-13, Sep. 2014. DOI: 10.1155/2014/217032.
- [5] S. Ju *et al.*, "Frequency Up-Converted Low Frequency Vibration Energy Harvester Using Trampoline Effect," *Journal of Physics: Conference Series*, vol. 476, p. 012089, Dec. 2013. DOI: 10.1088/1742-6596/476/1/012089.
- [6] S. Mathurosemontri, S. Thumsorn, S. Nagai, and H. Hamada, "Investigation of Friction and Wear Behavior of Polyoxymethylene/Poly(Lactic Acid) Blends," *Key Engineering Materials*, vol. 728, pp. 229-234, Jan. 2017. DOI: 10.4028/www.scientific.net/kem.728.229.
- [7] D. Hoffmann, B. Folkmer, and Y. Manoli, "Experimental Analysis of a Coupled Energy Harvesting System with Monostable and Bistable Configuration," *Journal of Physics: Conference Series*, vol. 557, p. 012134, Nov. 2014. DOI: 10.1088/1742-6596/557/1/012134.
- [8] D. Mallick, P. Podder, and S. Roy, "Wideband electromagnetic energy harvesting from ambient vibrations," *AIP Conference Proceedings*, vol. 1665, no. 1, p. 020001, Jun. 2015. DOI: 10.1063/1.4917572.
- [9] A. Munaz and G.-S. Chung, "An electromagnetic energy harvester based on multiple magnet scavenging power from low frequency vibration," *Microsystem Technologies*, vol. 23, no. 1, pp. 91-99, Jan. 2017. DOI: 10.1007/s00542-015-2732-z.